International Journal of Pharmaceutics 409 (2011) 252–259

Contents lists available at ScienceDirect

International Journal of Pharmaceutics

journal homepage: www.elsevier.com/locate/ijpharm

Pharmaceutical Nanotechnology

# Chitosan-*g*-poly(*N*-isopropylacrylamide) based nanogels for tumor extracellular targeting

Cunxian Duan[a], Dianrui Zhang[a,*], Feihu Wang[a], Dandan Zheng[a], Lejiao Jia[a], Feifei Feng[a], Yue Liu[a], Yancai Wang[a], Keli Tian[b], Fengshan Wang[c], Qiang Zhang[d]

[a] Department of Pharmaceutics, School of Pharmaceutical Sciences, Shandong University, 44 Wenhua Xilu, Jinan 250012, PR China
[b] Institute of Biochemistry and Molecular Biology, Medical School of Shandong University, 44 Wenhua Xi Road, Jinan 250012, PR China
[c] National Glycoengineering Research Center, School of Pharmaceutical Sciences, Shandong University, 44 Wenhua Xilu, Jinan 250012, PR China
[d] State Key Laboratory of Natural and Biomimetic Drugs, School of Pharmaceutical Sciences, Peking University, 38 Bei Xueyuan Road, Beijing 100083, PR China

ARTICLE INFO

*Article history:*
Received 23 January 2011
Accepted 20 February 2011
Available online 26 February 2011

*Keywords:*
Nanogels
Chitosan
*N*-isopropylacrylamide
Tumor extracellular pH
Oridonin

ABSTRACT

The principle objective of this research was to develop and characterize pH-responsive and biocompatible nanogels as a tumor-targeting drug delivery system. The nanogels were self-assembled from chitosan-based copolymers, chitosan-*graft*-poly(*N*-isopropylacrylamide) (CS-*g*-PNIPAm). The copolymers were synthesized via free radical copolymerization and characterized for their chemical structure by FT-IR and $^1$H NMR. These copolymers could be efficiently loaded with oridonin (ORI) and the characteristics of ORI-loaded nanogels were evaluated. Drug release researches indicated that the ORI-loaded nanogels displayed pH-dependent release behaviors. Based on MTT assay and cellular morphological analysis, the anti-tumor activity of ORI-loaded nanogels was higher at pH 6.5 than at pH 7.4. In conclusion, the obtained nanogels appeared to be of great promise in tumor extracellular pH targeting for ORI.



## 1. Introduction

Oridonin (ORI, Fig. 1), extracted from the Chinese traditional medicine *Rabdosia rubescens*, is a potent anticancer agent in Chinese traditional medicine. Both pharmacological experiments and clinical trials have demonstrated that ORI is effective against a variety of tumors and cancer cell types including: liver, prostate, breast and cervical cancer cells, non-small cell lung cancer cells, acute promyelocytic leukemia, and glioblastoma multiforme (Li et al., 1985; Zhang et al., 2003; Zhang and Ren, 2003). However, its clinical application against cancers has been impeded by its low therapeutic index induced by the poor solubility and nonspecifically systemic distribution. Hence, it is of great necessity to develop an alternative carrier of ORI for its referable application.

Recently, pH-responsive nanoparticles have been proposed as promising anti-cancer drug devices. Compared with other nanoparticles, these pH-sensitive nanoparticles create desirable switching carriers in release kinetics, from slow release while circulating to rapid release once target sites have been reached (Na et al., 2003; Lee et al., 2007; Yin et al., 2008; Garbern et al., 2010; Jiang et al., 2010). Amongst these particles, nanoparticles based on chitosan have been paid more and more attention due to their biocompatibility and non-toxicity (Cai et al., 2005; Fan et al., 2008; Li et al., 2009; Wu et al., 2010). Previous studies indicated that nanoparticles composed of NIPAAm and chitosan could achieve a pH-sensitive drug release and an enhanced anti-cancer activity under a slightly acidic environment (Fan et al., 2008; Li et al., 2009).

Therefore, in this research, efforts were devoted to exploit a pH-responsive nanoparticulate delivery system for ORI, intended to improve the therapeutic index. We synthesized CS-*g*-PNIPAm copolymers by free radical copolymerization using APS as an initiator and *N*,*N*-methylenebisacrylamide (MBA) as a cross-linking agent and applied them as the matrices of nanogels. The ORI-loaded nanogels were prepared by a self-assembly method and their physicochemical properties were studied. The in vitro release behaviors of ORI from the nanogels were determined at different pH values. Eventually, the in vitro anti-tumor activities were compared between the ORI solution and ORI-loaded nanogels at different pH values.

## 2. Materials and methods

### 2.1. Materials

*N*-Isopropylacrylamide (NIPAAm, Sigma) was purified by repeated re-crystallization from a mixture of toluene and hexane (1:5, v/v). Chitosan (medium $M_w$ = 200,000, degree of deacetylation: 96%), *N*,*N*-methylenebisacrylamide (MBA) and ammonium

* Corresponding author. Tel.: +86 531 8838 2015; fax: +86 531 8838 2015.
*E-mail address:* zhangdianrui2006@163.com (D. Zhang).

0378-5173/$ – see front matter © 2011 Elsevier B.V. All rights reserved.
doi:10.1016/j.ijpharm.2011.02.050

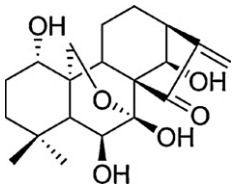


**Fig. 1.** Chemical structure of ORI.

persulfate (APS) were all purchased from Sigma and used without further purification. Oridonin (98%) was from Nanjing Zelang Pharmaceutical Co., Ltd. MTT and all other chemicals and reagents were obtained from Sigma. Hoechst 33342 and other biological reagents were purchased from Nanjing KeyGen Biotechnology Co., Ltd. All the other chemicals and solvents were of chromatographic and pharmaceutical grade.

### 2.2. Preparation of CS-g-PNIPAm copolymers

The copolymers of CS-*g*-PNIPAm were synthesized via a free radical copolymerization route (Mahdavinia et al., 2004). The copolymerization was carried out in a three-neck flask equipped with a stirrer, a reflux condenser, and a nitrogen inlet/outlet. An appropriate amount of CS (0.25 g) was first dissolved in 100 mL acetic acid solution (0.60%, v/v) under magnetic stirring in the flask. After CS solution was heated to 80 °C under nitrogen, APS (1.5 mL, $1.0 \times 10^{-2}$ mol/L) was added. The solution was stirred for 10 min before NIPAAm (1.0 g) and MBA (0.010 g) were added. The mixture was stirred for 3 h under nitrogen. The resulting product was dialyzed against distilled water and further freeze-dried.

### 2.3. Study of chemical structure

Fourier transform infrared (FT-IR, BRUKER VERTEX 70, German) and $^1$H nuclear magnetic resonance ($^1$H NMR, Inova-600, Varian, USA) measurements were utilized to characterize the chemical structure of CS-*g*-PNIPAm.

### 2.4. Preparation of ORI-loaded nanogels

ORI-loaded nanogels were prepared by a self-assembly method (Wang et al., 2007). Briefly, the copolymers (500 mg) and ORI (50 mg) were dispersed in 50 mL distilled water. And the dispersion was sonicated using a probe-type sonifier (JY92-Ultrasonic Processor Xinzhi, Linbo, Co., Ltd., China) at 100 W in an ice bath for 2 min. The resultant ORI-loaded nanogels were collected by centrifugation and lyophilized for storage and use.

An exactly weighted amount of the ORI-loaded nanogels was hydrolyzed in 1 mol/L HCl at 60 °C for 1 h and the content of total drug was determined using high-performance liquid chromatography (HPLC) analysis system (Agilent, USA). Free ORI was separated from the ORI-loaded nanogels by ultracentrifugation at 4000 rpm for 20 min and the content was analyzed by the HPLC. The mobile phase, consisting of methanol/water (55:45, v/v), was delivered at a flow rate of 1.0 mL/min. Eluted compounds were detected at a wavelength of 238 nm. The standard curve for the quantification of ORI was linear over the range of 1.04–104 μg/mL with a correlation coefficient of 0.9997. Encapsulation efficiency and drug loading were calculated using the following equations: Encapsulation efficiency (%) = (weight of total drug − weight of free drug found)/weight of total drug × 100; drug loading (%) = (weight of total drug − weight of free drug found)/weight of drug-loaded nanoparticles × 100.

### 2.5. Characterizations of ORI-loaded nanogels

#### 2.5.1. Morphology and particle size measurement

The particle sizes of the ORI-loaded and unloaded nanogels were estimated by the dynamic light scattering (DLS) method using a Dawn Heleos, Wyatt QELS, and Optilab DSP instrument (Wyatt Technology Co., USA). The morphologies of the unloaded and ORI-loaded nanogels were observed by transmission electron microscope (TEM, Hitachi, Japan).

#### 2.5.2. Crystalline state

The crystalline state of materials was estimated using an X-ray diffractometer (D/max r-B, Rigaku, Japan). Analysis was performed on CS, CS-*g*-PNIPAm, ORI and the freeze-dried ORI-loaded nanogels to investigate modifications of internal structure after drug incorporation.

### 2.6. Drug release from nanogels

The in vitro release of ORI from the ORI-loaded nanogels was studied at different pH values (pH 7.4, 7.0, 6.5, 6.0 and 5.0). The lyophilized ORI-loaded nanogels (containing 1 mg ORI) were dispersed in 2 mL of different solutions, which was transferred to a dialysis membrane bag (molecular cutoff = 12 kDa). Then, the sample-containing bag was immersed in 30 mL of homogeneous solution and kept at 37 °C with continuously magnetic stirring. At selected time intervals, 1 mL of the release medium outside the dialysis bag was withdrawn and the equal volume of fresh buffer solution was added. The amount of ORI was finally determined using the HPLC method as previously described for the measurement of encapsulation efficiency. Each experiment was repeated in triplicate.

### 2.7. Cytotoxicity and cell morphology

#### 2.7.1. Cell culture

Human hepatocellular carcinoma cell line HepG2 cells, kindly supplied by the Department of Pharmacology, Shandong University, were cultured in RPMI 1640 containing 10% fetal bovine serum, 100 U/mL of penicillin and 100 μg/mL of streptomycin at 37 °C in a humidified incubator with an atmosphere of 5% $CO_2$.

#### 2.7.2. MTT assay

HepG2 cells were seeded in 96-well culture plates for 12 h and were then exposed to the blank or ORI-loaded nanogels at various concentrations for 24 h. Subsequently, 15 μL of MTT (5 mg/mL) was added to each well. After 4 h incubation, culture media were discarded and 150 μL of DMSO was added. The optical density (OD) was measured at 570 nm with a Microplate Reader. The cell inhibitory rate was calculated as follows: Inhibitory rate (%) = $(A_{570\ \text{control cells}} - A_{570\ \text{treated cells}})/A_{570\ \text{conttol cells}} \times 100$. The $IC_{50}$ value was defined as the drug concentration of 50% inhibition rate relative to controls.

The pH-sensitive cytotoxicities of free ORI and the ORI-loaded nanogels against HepG2 cells were measured by initially plating the cells in 96-well tissue culture dishes for 12 h at pH 6.5 or 7.4 and then exposing them to the free ORI solution or ORI-loaded nanogels at the same pH for 24 h, respectively.

#### 2.7.3. Observation of cell morphology

HepG2 cells were seeded in 6-well plates and allowed to grow overnight at different pH values (pH 6.5 and 7.4). The cells were then treated with the blank nanogels, free ORI solution and ORI-loaded nanogels for 24 h. Finally, the cellular morphologies were estimated using reverse fluorescence microscopy (Nikon, Japan).

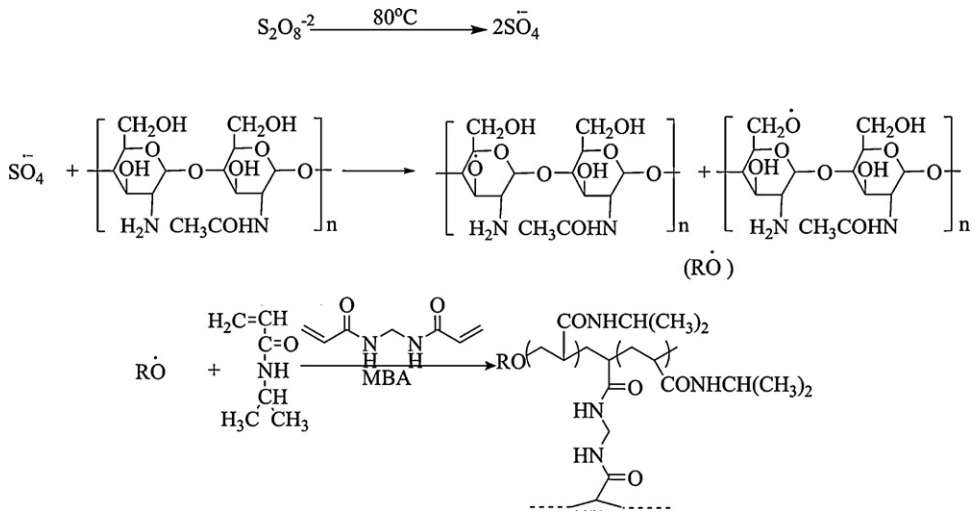


**Fig. 2.** The synthetic route for copolymers.

*2.7.4. Fluorescence image analysis*

HepG2 cells were seeded overnight into the 6-well culture plates and were treated with the blank nanogels, free ORI solution and ORI-loaded nanogels for 24 h at pH 6.5 or pH 7.4. The treated cells were washed twice with PBS and stained with Hoechst 33342 for 30 min and the stained cells were photographed using the reverse fluorescence microscopy (Nikon, Japan).

## 3. Results and discussion

### *3.1. Preparation and chemical composition of CS-g-PNIPAm copolymers*

The copolymers of CS-*g*-PNIPAm were prepared from the monomers of NIPAAm and CS by graft copolymerization in the presence of APS as a radical initiator and MBA as a cross-linking agent. The synthetic route was briefly illustrated in Fig. 2 (Mahdavinia et al., 2004; Zhang et al., 2007). APS was first decomposed to produce sulfate anion radicals under heating and then the radicals interacted with the hydroxyl groups of CS to form alkoxy radicals. These alkoxy radicals initiated the graft copolymerization of NIPAAm onto CS with MBA as a cross-linking agent (Mahdavinia et al., 2004; Zhang et al., 2007).

To identify the chemical structure of the synthesized copolymers, FT-IR and $^1$H NMR measurements were applied. The spectra of FT-IR and $^1$H NMR were shown in Figs. 3 and 4, respectively. The copolymers (Fig. 3a) showed new signals at 1385 and 1368 cm$^{-1}$ compared with CS (Fig. 3b), suggesting the presence of isopropyl groups in NIPAAm (Alvarez-Lorenzo et al., 2005; Don and Chen, 2005). In addition, the absorption bands of 1082 and 1032 cm$^{-1}$ in Fig. 3b were ascribed to $C_3$–OH and $C_6$–OH of CS. However, peak intensities of the absorption bands decreased in the FT-IR spectrum of the copolymers (Fig. 3a). This information revealed that the $C_3$–OH and/or $C_6$–OH of CS took part in graft reaction with NIPAAm (Zhang et al., 2007). Furthermore, the successful introduction of NIPAAm onto CS was verified by $^1$H NMR as well. $^1$H NMR spectrum of CS (Fig. 4b) displayed typical peaks including the peaks of protons on the carbon of CS (at 3.00–4.00 ppm) and a peak of methyl protons from partially acetylated chitosan (at 2.05 ppm), but the $^1$H NMR spectrum of the CS-*g*-PNIPAm copolymers displayed new peaks in Fig. 4a (Chiu et al., 2009). Obviously, two peaks (–CH–$CH_2$) at 1.00–2.20 ppm, a peak (–NH–CH<) at 3.90 ppm and a strong methyl group peak at 1.10 ppm all proved the existence of NIPAAm (Wei et al., 2006). In a word, it was believed that the graft copolymerization of NIPAAm onto CS did occur.

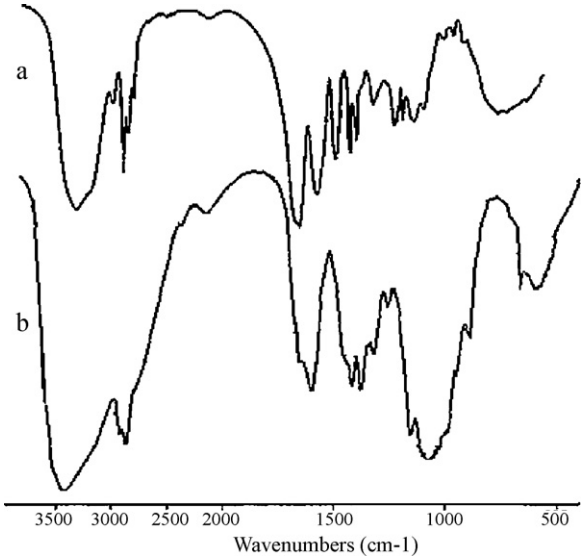


**Fig. 3.** FT-IR spectra of CS-*g*-PNIPAm (a) and CS (b).

### *3.2. Preparation and physicochemical characterization of ORI-loaded nanogels*

*3.2.1. Preparation of drug-loaded nanogels*

Since their self-assembly, the copolymers could self-assemble into particles and easily encapsulate poorly soluble drugs (Wang et al., 2007). The concept for the preparation of the drug-loaded nanogels was depicted in Fig. 5. After ORI and the copolymers were dispersed in water, the dispersion was sonicated using a probe-type sonifier, yielding the ORI-loaded nanogels with the drug encapsulation efficiency of 86.3% and the drug loading efficiency of 5.34%.

*3.2.2. Research of particle size and morphology*

The particle sizes and morphologies of the unloaded and drug-loaded nanogels were investigated by DLS and TEM experiments. The average hydrodynamic diameter ($R_d$) of the ORI-loaded nanogels was 99.6 nm, whereas the $R_d$ of the blank nanogels was 81.2 nm, indicating that ORI molecules were successfully encapsulated and that these entrapped ORI increased the size of the

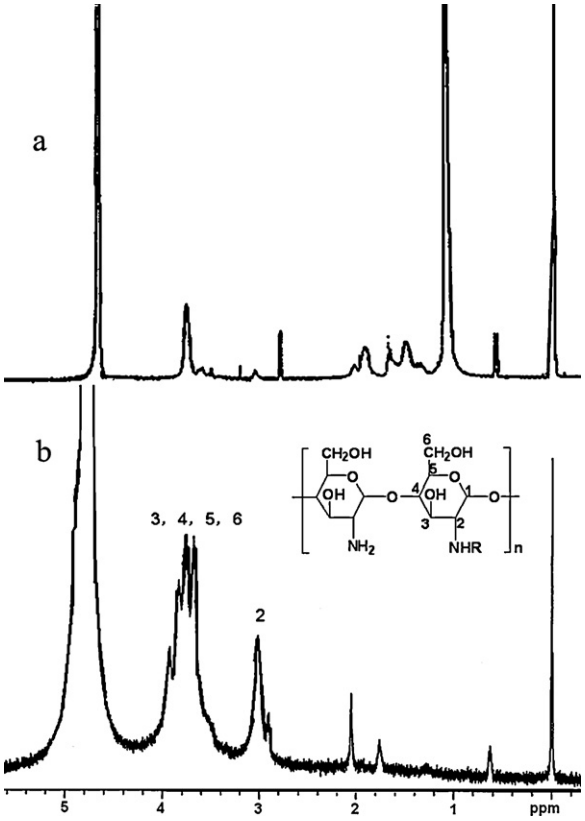


**Fig. 4.** $^1$H NMR spectra of CS-*g*-PNIPAm (a) and CS (b) in 1% DCl at 25 °C.

ORI-loaded nanogels. Importantly, as shown in Fig. 6, the resultant ORI-loaded nanogels had a relatively uniform size distribution and were approximately spherical and regular under TEM.

### 3.2.3. X-ray diffraction study

The physicochemical status of incorporated drug was very important for a drug delivery system to assess the interaction amongst different components during the fabrication process and to explain the relevant properties both in vitro and in vivo (Soo et al., 2002). The study on the crystallinity could help to ascertain the physicochemical status of incorporated drug. Fig. 7 exhibits the X-ray diffraction patterns of CS, CS-*g*-PNIPAm, ORI and the freeze-dried ORI-loaded nanogels. ORI displayed several intense peaks, while these characteristic peaks were not observed in the X-ray diffraction pattern of the drug-loaded nanogels. These results demonstrated that ORI was either molecularly dispersed or distributed in an amorphous state in the nanogels, which might be expected to increase the solubility and bioavailability of ORI (Xing et al., 2007).

Besides, although two peaks at $2\theta = 11.58°$ and 20.20° were observed in the X-ray diffraction pattern of CS (Fig. 7a), only one broad peak was observed at $2\theta = 22.28°$ in that of CS-*g*-PNIPAm (Fig. 7b), which indicated that the copolymers of CS-*g*-PNIPAm were amorphous but CS was crystalline. The X-ray diffraction analyses of CS and CS-*g*-PNIPAm further confirmed the occurrence of graft copolymerization.

## 3.3. In vitro release studies

ORI release profiles from the nanogels at various pH values (pH 7.4, 7.0, 6.5, 6.0 and 5.0) were depicted in Fig. 8. From the figures, we could find that pH had an effect on the drug release from the CS-

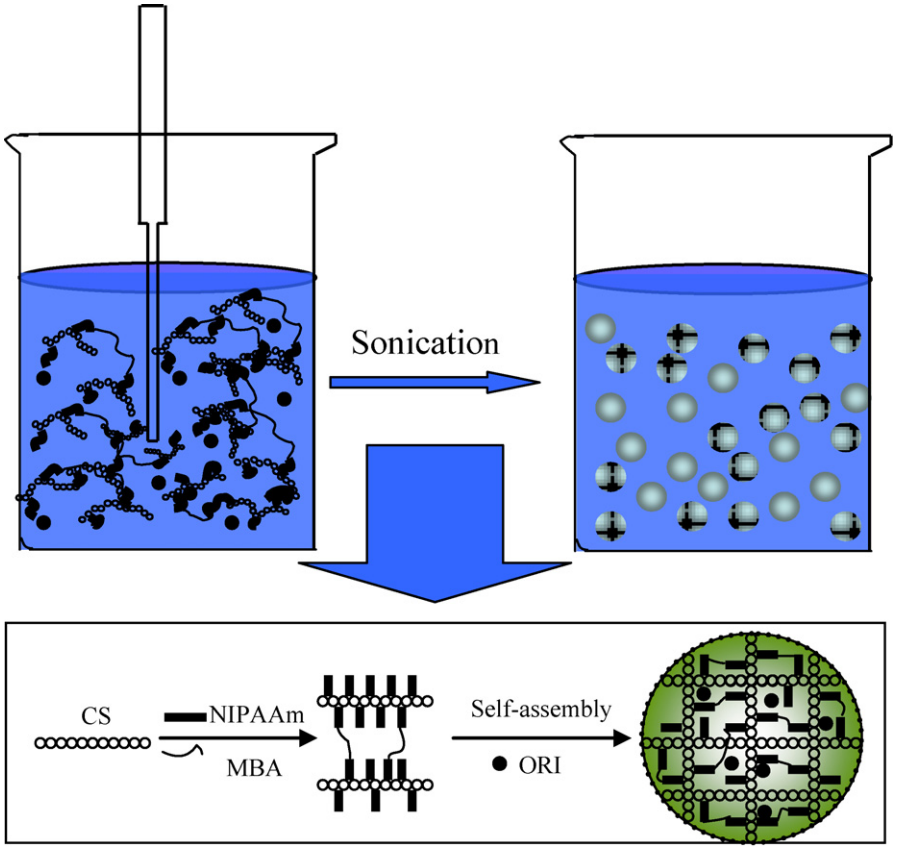


**Fig. 5.** The concept of the preparation of ORI-loaded nanogels.

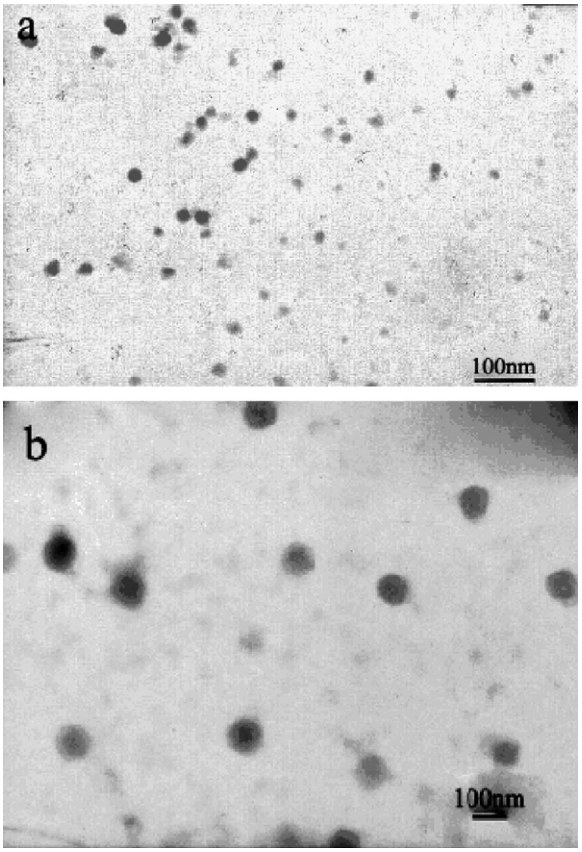


**Fig. 6.** TEM images of the unloaded (a) and ORI-loaded nanogels (b).

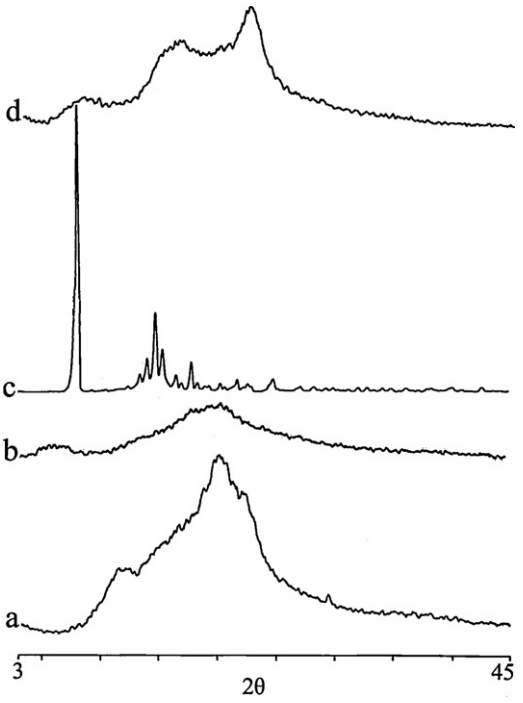


**Fig. 7.** XRD spectra of CS (a), CS-*g*-PNIPAm (b), ORI (c) and the freeze-dried ORI-loaded nanogels (d).

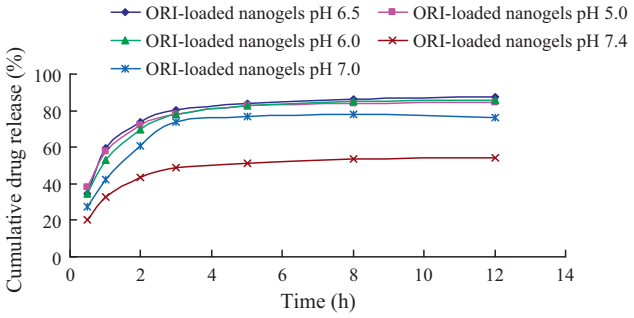


**Fig. 8.** Release profiles of ORI from the ORI-loaded nanogels.

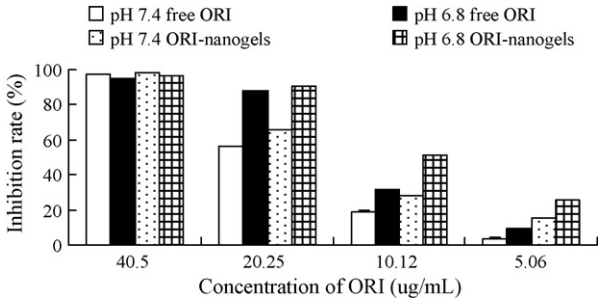


**Fig. 9.** Cytotoxic activities of the ORI-loaded nanogels and free ORI on HepG2 cells after 24 h of treatment at different pH values. Data are mean ± SD ($n = 4$).

*g*-PNIPAm nanogels. The drug release was slow at pH 7.4 while it was accelerated at low pH. The cumulative release rates drastically increased from about 50% at pH 7.4 to more than 80% at pH 6.5, 6.0 and 5.0, owing in part to the ionization of CS (Fan et al., 2008; Li et al., 2009; Langerman et al., 1990).

### 3.4. In vitro anticancer activities

The anti-tumor activities of the free ORI dissolved in dimethyl sulfoxide (DMSO, 0.1%), black nanogels, and ORI-loaded nanogels were evaluated using MTT method. The tests for black nanogels indicated that the nanogels with the concentrations from 0.025 to 5.0 mg/mL had no apparent harm on the proliferation of HepG2 cells after 24 h incubation (Data were not listed). As shown in Fig. 9, the cytostatic activities of both the ORI-loaded nanogels and ORI solution increased in parallel with drug concentrations. Besides, the ORI-loaded nanogels showed a higher cellular cytotoxicity relative to the ORI solution at the same pH. At pH 7.4, the mean apoptotic population of the HepG2 cells treated with the ORI solution was 56.11 ± 0.04%, 18.81 ± 0.52% and 3.37 ± 0.96%, while for the ORI nanogels treated cells apoptosis was increased to 66.07 ± 0.02%, 28.34 ± 0.15% and 15.49 ± 0.22% after 24 h of exposure to 20.25, 10.12 and 5.06 μg/mL, respectively ($p < 0.05$). The enhanced cytotoxicity might be attributed to two factors, the enhanced internalization of nanoparticles via endocytosis or phagocytosis and the high drug uptake by cells through the active interaction between particles and the cells induced by the PNIPAm chains in the nanogels (Na et al., 2003; Chung et al., 2000).

In addition, in the case of the ORI-loaded nanogels, anticancer cytotoxic activity against HepG2 cells was significantly increased at pH 6.5 compared to that at pH 7.4 ($p < 0.05$). The $IC_{50}$ value for the ORI-loaded nanogels was also found to be pH-dependent. The value was 8.86 μg/mL at pH 6.5 compared with that of 13.19 μg/mL at pH 7.4. This pH-responsive cytotoxicity might be due to the pH-sensitive rapid drug release at a low pH condition. Interestingly, we discovered that ORI displayed a pH-responsive cytotoxic activity as well and this phenomenon had not been discovered before. The

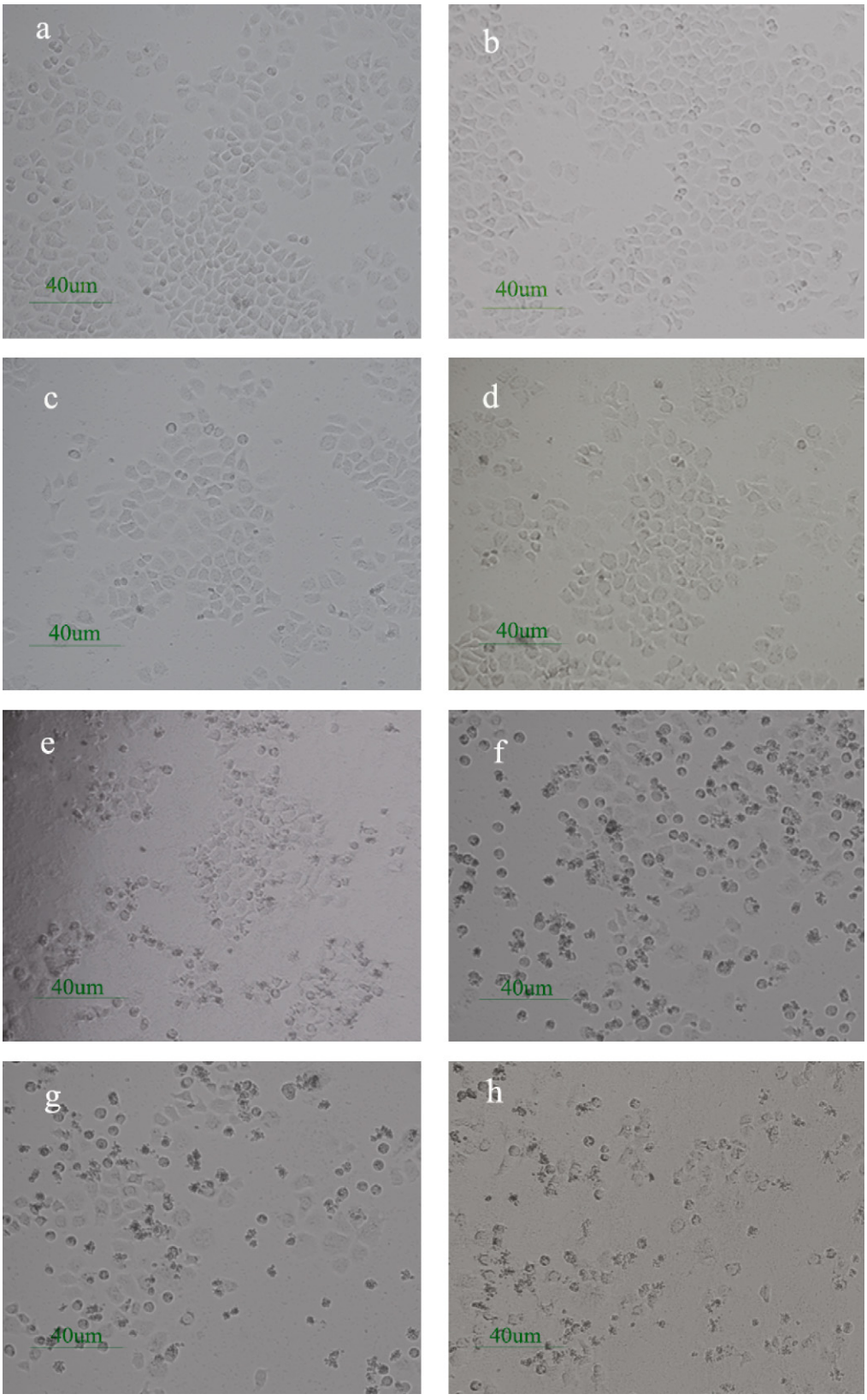


**Fig. 10.** Cellular morphologies of HepG2 cells at different pHs: (a) control at pH 7.4, (b) control at pH 6.5, (c) the unloaded nanogels at pH 7.4, (d) the unloaded nanogels at pH 6.5, (e) free ORI at pH 7.4, (f) free ORI at pH 6.5, (g) the ORI-loaded nanogels at pH 7.4, and (h) the ORI-loaded nanogels at pH 6.5.

mechanism of increased anticancer activity under an acidic environment was still unknown. It might associate with the different molecular conformation of ORI or the activated metabolic pathways under acidic environments (Fukamachi et al., 2010).

### 3.5. Microscopic observations

Reverse fluorescence microscopy was used to investigate the changes in cellular morphology. Figs. 10 and 11 show the mor-

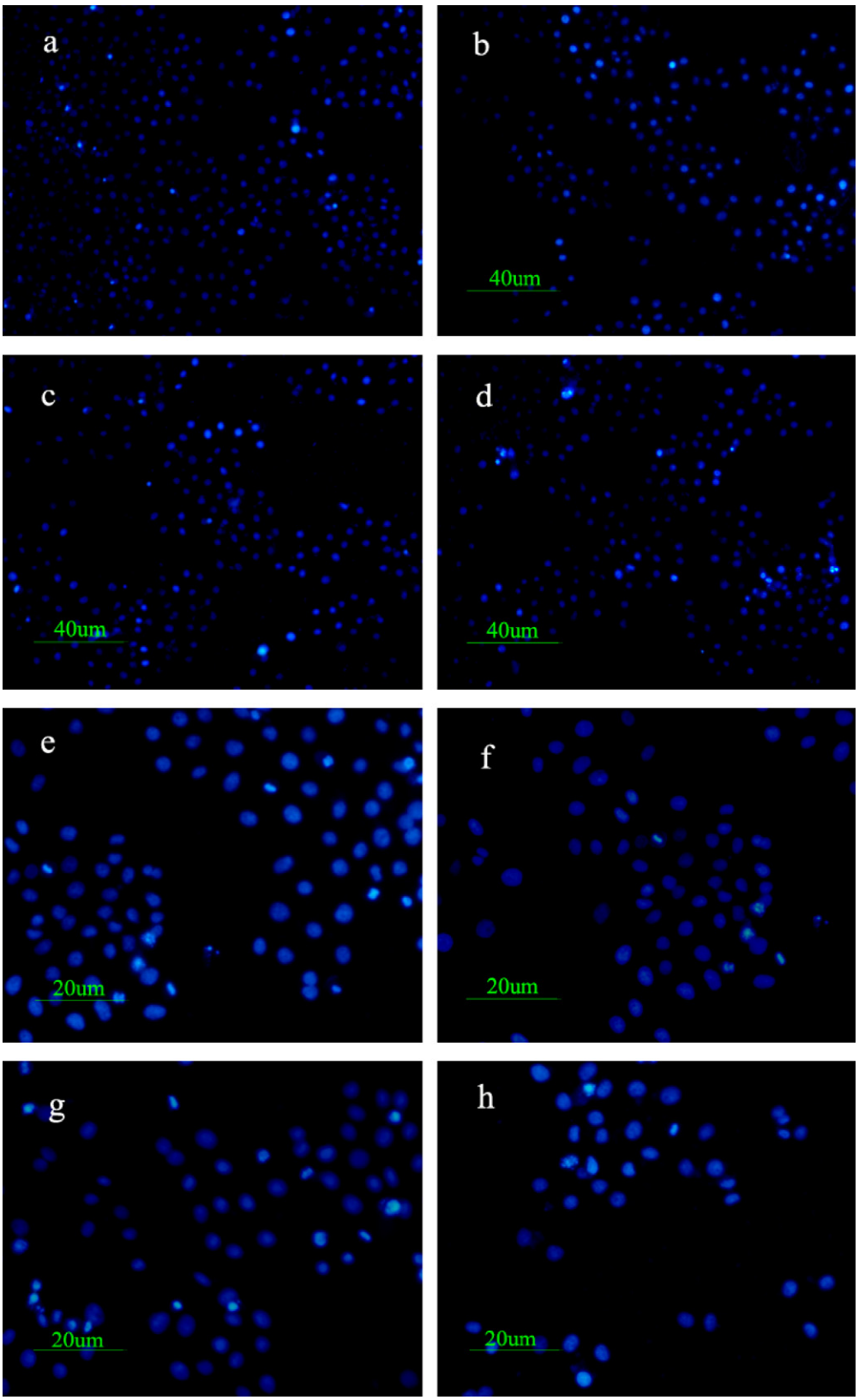


**Fig. 11.** Nuclear morphologies of HepG2 cells using Hoechst 33342 staining at pHs: (a) control at pH 7.4, (b) control at pH 6.5, (c) the unloaded nanogels at pH 7.4, (d) the unloaded nanogels at pH 6.5, (e) free ORI at pH 7.4, (f) free ORI at pH 6.5, (g) the ORI-loaded nanogels at pH 7.4, and (h) the ORI-loaded nanogels at pH 6.5.

phological images obtained after 24 h of treatment with different samples at different pH values (pH 7.4 or 6.5). The cells were polygonal, cellular skeletons were clear and nucleoli were evident under control conditions (Fig. 10a and b). No apparent signs of morphological damage to HepG2 cells were observed upon the treatment with the blank nanogels for 24 h at the concentration of 5.0 mg/mL (Fig. 10c and d). As shown in Fig. 10e–h, however, morphological changes were observed, including cell shrinkage and rounding

after 24 h exposure to both the free ORI solution and ORI-loaded nanogels. Apart from these, at the same pH the number of normal cells in the ORI nanogels was lower than in the ORI solution. In the case of ORI nanogels, the number of normal cells decreased with decreasing pH. These results were further confirmed by Hoechst 33342 staining assay. From Fig. 11, the nuclei of the untreated HepG2 cells were round and homogeneously stained (Fig. 11a and b), whereas those of the cells treated with the ORI solution and ORI-loaded nanogels exhibited chromatin condensation and nuclear fragmentation in Fig. 11e–h. For the ORI-loaded nanogels, normal nuclei at pH 6.5 (Fig. 11g) were less than at pH 7.4 (Fig. 11h). Besides, the ORI-loaded nanogels markedly reduced the number of normal nuclei, compared with the ORI solution at the same pH. The above results were agreed well with the results of MTT tests.

## 4. Conclusion

Copolymers, CS-*g*-PNIPAm, were synthesized in an aqueous solution via free radical copolymerization using APS as the radical initiator and MBA as the crosslinking agent. They could self-assemble into nanogels and a hydrophobic drug, ORI, could be successfully encapsulated. In vitro drug release researches indicated that ORI-loaded nanogels exhibited a pH-triggered fast drug release under a slightly acidic condition. Moreover, both the MTT assay and cellular morphological analysis demonstrated that the ORI-loaded nanogels could enhance the anti-tumor activity under an acidic environment. No significant cytotoxicity, however, was observed with the blank carriers themselves. Therefore, this nanogels-based delivery system might be exploitable in tumoral acidic extracellular pH targeting for hydrophobic anticancer drugs.

## Acknowledgements

This work was supported by the National Nature Science Foundation of China, No. 81073054 and the National Basic Research Program of China (973 Program), No. 2009CB930300.

## References

Alvarez-Lorenzo, C., Concheiro, A., Dubovik, A.S., Grinberg, N.V., Burova, T.V., Grinberg, V.Y., 2005. Temperature-sensitive chitosan-poly(*N*-isopropylacrylamide) interpenetrated networks with enhanced loading capacity and controlled release properties. J. Control. Release 102, 629–641.

Cai, H., Zhang, Z.P., Sun, P.C., He, B.L., Zhu, X.X., 2005. Synthesis and characterization of thermo- and pH- sensitive hydrogels based on Chitosan-grafted *N*-isopropylacrylamide via γ-radiation. Radiat. Phys. Chem. 74, 26–30.

Chiu, Y.L., Chen, S.C., Su, C.J., Hsiao, C.W., Chen, Y.M., Chen, H.L., Sung, H.W., 2009. pH-triggered injectable hydrogels prepared from aqueous *N*-palmitoyl chitosan: in vitro characteristics and in vivo biocompatibility. Biomaterials 30, 4877–4888.

Chung, J.E., Yokoyama, M., Okano, T., 2000. Inner core segment design for drug delivery control of thermo-responsive polymeric micelles. J. Control. Release 65, 93–103.

Don, T.M., Chen, H.R., 2005. Synthesis and characterization of AB-crosslinked graft copolymers based on maleilated chitosan and *N*-isopropylacrylamide. Carbohydr. Polym. 61, 334–347.

Fan, L., Wu, H., Zhang, H., Li, F., Yang, T., Gu, C., Yang, Q., 2008. Novel super pH-sensitive nanoparticles responsive to tumor extracellular pH. Carbohydr. Polym. 73, 390–400.

Fukamachi, T., Chiba, Y., Wang, X., Saito, H., Tagawa, M., Kobayashi, H., 2010. Tumor specific low pH environments enhance the cytotoxicity of lovastatin and cantharidin. Cancer Lett. 297, 182–189.

Garbern, J.C., Hoffman, A.S., Stayton, P.S., 2010. Injectable pH- and temperature-responsive poly(*N*-isopropylacrylamide-co-propylacrylic acid) copolymers for delivery of angiogenic growth factors. Biomacromolecules 11, 1833–1839.

Jiang, J., Hua, D., Tang, J., 2010. One-pot synthesis of pH- and thermo-sensitive chitosan-based nanoparticles by the polymerization of acrylic acid/chitosan with macro-RAFT agent. Int. J. Biol. Macromol. 46, 126–130.

Langerman, L., Chaimsky, G., Golomb, E., Tverskoy, M., Kook, A.I., Benita, S., 1990. A rabbit model for evaluation of spinal anesthesia: chronic cannulation of the subarachnoid space. Anesth. Analg. 71, 529–535.

Lee, E.S., Oh, K.T., Kim, D., Youn, Y.S., Bae, Y.H., 2007. Tumor pH-responsive flower-like micelles of poly(L-lactic acid)-b-poly(ethylene glycol)-b-poly(L-histidine). J. Control. Release 123, 19–26.

Li, F., Wu, H., Zhang, H., Li, F., Gu, C., Yang, Q., 2009. Antitumor drug Paclitaxel-loaded pH-sensitive nanoparticles targeting tumor extracellular pH. Carbohydr. Polym. 77, 773–778.

Li, X.T., Lin, C., Li, P.Y., Zhang, T.M., 1985. The comparisons of sensibility of seven kinds of human carcinoma cell lines to the oridonin. Acta Pharm. Sci. 20, 243–246.

Mahdavinia, G.R., Pourjavadi, A., Hosseinzadeh, H., Zohuriaan, M.J., 2004. Modified chitosan 4. Superabsorbent hydrogels from poly(acrylic acid-co-acrylamide) grafted chitosan with salt- and pH-responsiveness properties. Eur. Polym. J. 40, 1399–1407.

Na, K., Lee, E.S., Bae, Y.H., 2003. Adriamycin loaded pullulan acetate/sulfonamide conjugate nanoparticles responding to tumor pH: pH-dependent cell interaction, internalization and cytotoxicity in vitro. J. Control. Release 87, 3–13.

Soo, P.L., Luo, L., Maysinger, D., Eisenberg, A., 2002. Incorporation and release of hydrophobic probes in biocompatible polycaprolactone-*block*-poly(ethylene oxide) micelles: implications for drug delivery. Langmuir 18, 9996–10004.

Wang, Y., Liu, L., Weng, J., Zhang, Q., 2007. Preparation and characterization of self-aggregated nanoparticles of cholesterol-modified *O*-carboxymethyl chitosan conjugates. Carbohydr. Polym. 69, 597–606.

Wei, H., Zhang, X.Z., Cheng, H., Chen, W.Q., Cheng, S.X., Zhuo, R.X., 2006. Self-assembled thermo- and pH responsive micelles of poly(10-undecenoic acid-b-*N*-isopropylacrylamide) for drug delivery. J. Control. Release 116, 266–274.

Wu, W., Shen, J., Banerjee, P., Zhou, S., 2010. Chitosan-based responsive hybrid nanogels for integration of optical pH-sensing, tumor cell imaging and controlled drug delivery. Biomaterials 31, 8371–8381.

Xing, J., Zhang, D., Tan, T., 2007. Studies on the oridonin-loaded poly(D,L-lactic acid) nanoparticles in vitro and in vivo. Int. J. Biol. Macromol. 40, 153–158.

Yin, H., Lee, E.S., Kim, D., Lee, K.H., Oh, K.T., Bae, Y.H., 2008. Physicochemical characteristics of pH-sensitive poly(L-histidine)-b-poly(ethylene glycol)/poly(L-lactide)-b-poly(ethylene glycol) mixed micelles. J. Control. Release 126, 130–138.

Zhang, D.R., Ren, T.C., 2003. Pharmaceutical progress of oridonin. Chin. Pharm. J. 38, 817–820.

Zhang, J., Wang, Q., Wang, A., 2007. Synthesis and characterization of chitosan-*g*-poly(acrylic acid)/attapulgite superabsorbent composites. Carbohydr. Polym. 68, 367–374.

Zhang, J.X., Han, Q.B., Zhao, A.H., Sun, H.D., 2003. Diterpenoids from *Isodon japonica*. Fitoterapia 74, 435–438.